RSC Advances

ROYAL SOCIETY OF CHEMISTRY

www.rsc.org/advances

Journal Name

RSCPublishing

COMMUNICATION

Lumazine synthase protein cage nanoparticles as modular delivery platforms for targeted drug delivery

Cite this: DOI: 10.1039/x0xx00000x

Junseon Min, Soohyun Kim, Jisu Lee and Sebyung Kang[a]

Received ooth January 2012,
Accepted ooth January 2012

DOI: 10.1039/x0xx00000x

www.rsc.org/

Lumazine synthase protein cage nanoparticle isolated from *Aquifex aeolicus* (AaLS) is developed as a modular delivery nanoplatform that genetically acquires either tumor vasculature targeting peptides or hepatocellular carcinoma cell surface targeting peptides on its surface. The targeting peptide bearing AaLS effectively delivers its cargoes to their target cancer cells.

The targeted delivery of diagnostic or/and therapeutic reagents to desired sites is a challenging, but promising, task for the early diagnosis of diseases as well as effective and localized treatment of diseases. A variety of inorganic or organic nanoparticles, including metal nanoparticles,[1, 2] micelles,[3, 4] polymers,[5-7] liposomes,[7-9] and protein cages,[10, 11] have been investigated as efficient delivery vehicles for diagnostic or/and therapeutic reagents because they have great potential to improve the pharmacological properties of drugs and maximize the localized treatment of diseases.[12] Especially, protein cages, such as ferritins,[13-17] small heat shock proteins,[18-20] and viral capsids,[21-26] are promising nanoplatform candidates for efficient delivery systems because they have uniform size and structure as well as high biocompatibility and biodegradability.[10]

To achieve the maximum usage of the protein cage as an effective delivery system for therapeutic or/and imaging reagents, it is necessary to develop a modular delivery template that can acquire multiple functions on demand. The modular delivery template can adapt various targeting ligands and selectively carry diagnostic or/and therapeutic cargos to target diseases, including cancers, in multiple ways using a mixing-and-matching strategy. To aim this, modular delivery template should have genetic and chemical plasticity amenable to simultaneously introducing multiple cell-specific targeting ligands, diagnostic agents, and their corresponding drugs at desired sites depending on its purpose.

Here, we developed lumazine synthase, isolated from the hyperthermophile *Aquifex aeolicus*, (AaLS) as a modular delivery nanoplatform for the targeted delivery of diagnostic and/or therapeutic molecules depending on target cancer cells and evaluated their efficacies (Scheme 1).

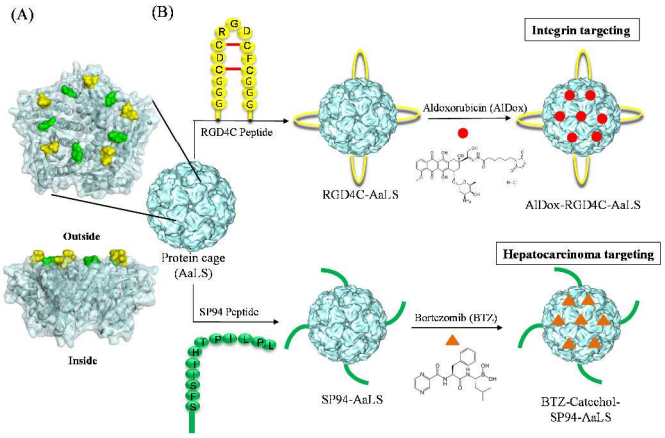

Scheme 1 (A) Surface and ribbon representations of the AaLS pentamer (top and side views). The positions where RGD4C peptides (yellow) and SP94 peptides (green) were introduced were indicated. (B) Schematic representation of utilizing AaLS as a versatile modular template for delivery nanoplatform. The RGD4C- or SP94 peptides were genetically introduced onto the exterior surface of the assembled AaLS to target surface integrins or hepatocarcinoma surface markers. Their corresponding anticancer drugs, aldoxorubicin (AlDox) and bortezomib (BTZ), were chemically attached to each AaLS.

AaLS consists of 60 identical subunits that form an icosahedral capsid architecture (T = 1 state) with 15.4-nm exterior and 9-nm interior diameters.[27] Within the cell, AaLS catalyzes the penultimate step in riboflavin biosynthesis.[28] Outside of the cell, its hollow spherical architecture has been used as a template for the encapsulation of cargo proteins, such as green fluorescent proteins[29, 30] and HIV proteases[31], and fabrication of uniform layer-by-layer (LbL) assemblies using non-covalent interactions between surface-displayed hexahistidine and Ni-NTA of AaLS[32]. These studies successfully demonstrated the encapsulation capability of AaLS and surface presentation of ligands, which represent the great potential of AaLS as a versatile delivery vehicle.

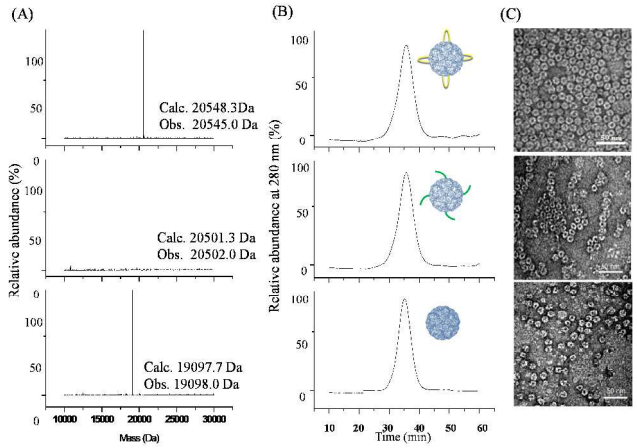

Fig. 1 Characterization of RGD4C- and SP94-AaLS. (A) Molecular mass measurements of dissociated subunits of wt (bottom), SP94- (middle) and RGD4C-AaLS (top). Calculated and observed molecular masses were indicated. (B) Size exclusion elution profiles of wt (bottom), SP94- (middle) and RGD4C-AaLS (top). (C) Transmission electron microscopic images of negatively stained wt (bottom), SP94- (middle) and RGD4C-AaLS (top) with 2% uranyl acetate.

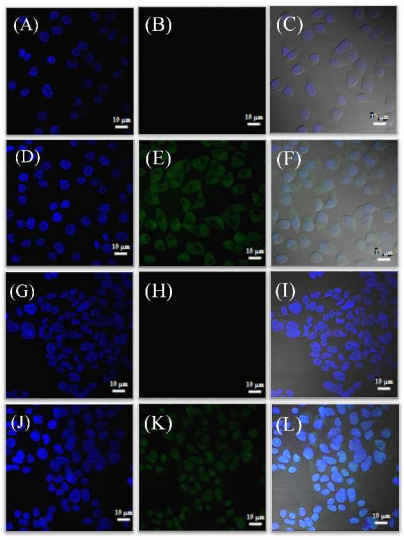

Fig. 2 Fluorescent microscopic images of KB cells (A-F) treated with fAaLS (A-C) and fRGD4C-AaLS (D-F). Fluorescent microscopic images of HepG2 cells (G-L) treated with fAaLS (G-I) and fSP94-AaLS (J-L). DAPI (left rows), fluorescein (middle rows) and merged (right rows) were presented. The fRGD4C- and fSP94-AaLS and nuclei were visualized as green and blue, respectively.

To develop a versatile drug delivery nanoplatform, we genetically introduced two different cell-targeting peptides independently (Scheme 1). We chose RGD4C and SP94 peptides to function as specific cell-targeting peptides. The RGD4C peptide selectively binds to integrin αvβ3 receptors, which are overexpressed on the surface of activated endothelial cells during pathological angiogenesis, and the SP94 peptide specifically binds to the surface receptor of hepatocellular carcinoma (HCC) cells.[33]

Because the crystal structure of AaLS is known, we selectively incorporated targeting peptides to desired positions. We started with a genetically engineered AaLS construct (R108C), which has one extra cysteine per subunit, for later site-selective modifications with either imaging or/and therapeutic molecules. Subsequently, we inserted the RGD4C peptide with extra linker sequences (GGGCDCRGDCFCASGGG) to the position between residues 70 and 71, where the exterior loop is formed,[27] allowing RGD4C peptides to adopt an active cyclic form through intramolecular disulfide bonds. In parallel, we introduced the SP94 peptide (SFSIIHTPILPL) to the C-terminal end of AaLS because the C-termini are on the exterior surface based on atomic resolution structural information[27] and the linear form of SP94 peptide being the most active.[33, 34]

Both the RGD4C peptide-inserted (RGD4C-AaLS) and SP94 peptide-inserted AaLS (SP94-AaLS) with cysteine mutations were each overexpressed in *E. coli*, purified, and characterized using various biophysical methods. Introductions of desired peptide sequences were confirmed by DNA sequencing. Electrospray ionization time-of-flight mass spectrometry (ESI-TOF MS) analysis indicated that the subunit masses of RGD4C-AaLS, SP94-AaLS, and wild-type (wt) AaLS were 20545.0 Da, 20502.0 Da, and 19098.0 Da, respectively; these values corresponded to the predicted masses of 20548.3 Da, 20501.2 Da, and 19097.7 Da, respectively (Fig. 1A). Approximately a 3.3-Da difference between the observed and calculated subunit masses of RGD4C-AaLS was observed, which might have resulted from the loss of protons when intramolecular disulfide bonds form to make a cyclic RGD4C peptide (4 cysteine residues). These results demonstrated that RGD4C and SP94 peptides were properly introduced to the target positions in AaLS. Purified RGD4C- and SP94-AaLS eluted at the same position as wt AaLS in size exclusion chromatography (SEC), suggesting that the genetic insertions of the targeting peptides did not significantly alter the overall size and shape of the cage architectures (Fig. 1B). Transmission electron microscopic (TEM) images of negatively stained RGD4C- and SP94-AaLS confirmed their intact cage architectures with a uniform size distribution of approximately 16 nm (Fig. 1C). These results demonstrated the successful incorporation of either RGD4C or SP94 peptides into the exterior loop or C-terminal end of AaLS by rational design.

To evaluate the capability of targeted delivery of RGD4C- and SP94-AaLS, we attached 5-(and 6)-carboxy-fluorescein-succinimidyl ester (NHS-fluorescein) to RGD4C- or SP94-AaLS via an N-hydroxysuccinimide ester (NHS) reaction with primary amines. After the reactions were completed, unreacted NHS-fluorescein was removed from the modified AaLS by SEC and the conjugation was confirmed by subunit mass analyses using ESI-TOF MS, UV/Vis spectrophotometer, and SEC (Figs. S1 and S2).

Fluorescence microscopy was used to determine whether fRGD4C- or fSP94-AaLS could bind selectively to their target cells, KB or HepG2 cells (Fig. 2). While each fRGD4C-AaLS and fSP94-AaLS efficiently bound to KB cells and HepG2 cells, respectively (Figs. 2E and 2K), fAaLS could not bind to cells without any targeting peptides (Figs. 2B and 2H). Furthermore, we switched the target cells (fRDG4C-AaLS toward HepG2 cells and fSP94-AaLS toward KB cells) to test target specificity and significant binding was not observed (Fig. S3), indicating that each RGD4C- and SP94-AaLS efficiently recognizes its unique target ligand on specific cancer cells and bind to them tightly. These results clearly suggest that both cell targeting and imaging functionalities can be simultaneously incorporated into the AaLS modular template for use as a target-specific diagnostic probe.

To evaluate the reactivity of the cysteine residue introduced for attaching prodrugs or/and diagnostic reagents, the purified RGD4C- and SP94-AaLS were treated with activated fluorescein-5-maleimide (F5M). F5M-conjugated AaLS was separated from unreacted F5M by SEC, and the content of conjugation was determined by subunit mass analyses using ESI-TOF MS (Figs. S4 and S5). Both RGD4C- and SP94-AaLS were clearly labeled with only one F5M without any side reactions (Fig. S4A and S5A). The SEC elution profiles of

the F5M-conjugated RGD4C- or SP94-AaLS were the same as those of the untreated RGD4C- or SP94-AaLS, indicating that F5M labeling does not cause any aggregation or disassembly of AaLS (Figs. S4B and S5B).

To load two different corresponding chemotherapeutic cargoes to AaLS based on their target cancer cells, we used the following two approaches: a direct conjugation of prodrugs and a non-covalent complexation of drugs and drug-capturing ligands. For RGD4C-AaLS, aldoxorubicin (AlDox) was directly conjugated to the cage via a thiol-maleimide Michael-type addition. AlDox is a 6-maleimidocaproyl hydrazone derivative prodrug of doxorubicin,[35] which can inhibit tumor angiogenesis and metastasis and exhibit high cytotoxic effects on high integrin αvβ3-expressing cancer cells.[36] The hydrazone linkage can be efficiently cleaved for drug release upon a decrease in pH to approximately pH 5.5.[35] The successful conjugation of AlDox and degree of conjugation were evaluated by a UV/Vis spectrophotometer (Fig. S6A). UV/Vis analysis revealed that the AlDox contents were 0.81 per protein subunit, translating to 48 AlDox molecules per RGD4C-AaLS (60 subunits). A time-dependent release study of AlDox from AlDox-RGD4C-AaLS at pH 5.5 showed that approximately 65% of AlDox was released at 15 h and the rest remained even after 48 h (Fig. S6B).

We chose bortezomib (BTZ) as an anticancer drug in the case of SP94-AaLS as it is known to effectively inhibit proteasome activity in HCC cells.[37, 38] To deliver BTZ to the target HCC, catechol (benzene 1,2-diol) ligands were first attached to SP94-AaLS, on which BTZ could be captured through boronic acid-diol complexation as previously described.[39] First, we covalently conjugated the bifunctional N-(3,4-dihydroxyphenethyl)-3-maleimido-propanamide (Catechol-Mal) to SP94-AaLS via a thiol-maleimide Michael-type addition (Fig. S7). Subsequently, BTZ was introduced and captured through non-covalent boronic acid-diol complexation to the Catechol-anchored SP94-AaLS (Catechol-SP94-AaLS). To study the interactions between BTZ and Catechol-SP94-AaLS, we used the same indirect methods as previously reported.[39] Pyrene-1-boronic acid (PBA), an analogue of BTZ, was readily evaluated using a UV/Vis spectrophotometer because of its strong absorption at approximately 340 nm. According to the measured absorbance at 340 nm, we effectively measured the binding of PBA to Catechol-SP94-AaLS and release of PBA from complexes (Figs. S6C–D). The boronic acid-diol complexation, such as the PBA/BTZ-catechol complex, is pH-dependent.[40] Thus, the complex stabilized under neutral and alkaline conditions, but dissociated in acidic environments. PBA-catechol complex formation at pH 9.0 was confirmed and quantified by UV/Vis absorbance at 340 nm, providing that 0.72 PBA content was attached per protein subunit, which translates to 43 PBA molecules per SP94-AaLS complex. Furthermore, the time-dependent release study of PBA from PBA-Catechol-SP94-AaLS complexes at pH 5.5 showed that most PBA was released within 12 h (Fig. S6D).[39] The site-specific loadings of two distinct drugs, AlDox or BTZ, by either direct conjugation or boronic acid-diol complexation suggest that the targeting peptide bearing AaLS has potential to be used as a versatile modular nanocarrier for therapeutic cargo on demand.

To examine the efficacy of the delivered drugs by RGD4C- or SP94-AaLS, 3-(4,5-dimethylthiazol-2-yl)-2,5-diphenyltetrazolium bromide (MTT) cell viability assays were performed (Fig. 3). The KB cells and HepG2 cells were treated with AlDox-RGD4C-AaLS and BTZ-Catechol-SP94-AaLS, respectively, for 3 h. The free drugs (AlDox and BTZ) and RGD4C- or SP94-AaLS were also treated in parallel to serve as positive and negative controls. Three hours later, cells were washed with fresh media and further cultured for 24 h and their viability was measured to investigate the cytotoxicity of

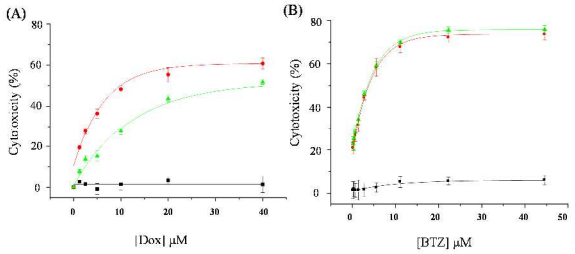

Fig. 3 MTT cell viability assay. (A) Dose-dependent cytotoxicity profiles of AlDox-RGD4C-AaLS (red, circles), free AlDox (green, triangles), and RGD4C-AaLS (black, squares) toward KB cells. (B) Dose-dependent cytotoxicity profiles of BTZ-Catechol-SP94-AaLS (red, circles), free BTZ (green, triangles), and Catechol-SP94-AaLS (black, squares) toward HepG2 cells.

delivered drugs. The cytotoxic effects of AlDox-RGD4C-AaLS on KB cells significantly increased in a dose-dependent manner and were higher than that of free AlDox, whereas RGD4C-AaLS without AlDox had no significant effect on cell viability (Figs. 3A and S8A). The enhanced cytotoxicity of AlDox-RGD4C-AaLS may be due to integrin αvβ3 receptor-mediated endocytosis, which transports increased amounts of AlDox into the KB cells. The cytoxicity of HepG2 cells treated with BTZ-Catechol-SP94-AaLS also increased in a dose-dependent manner, similar to that of free BTZ; SP94-AaLS without BTZ had almost no cytotoxicity on the cells (Figs. 3B and S8B). The similarity of cytotoxicity between them might be a result of BTZ release from BTZ-catechol conjugates. In spite of their similar cytotoxic effect, SP94-AaLS could promote uptake of BTZ within the cells, providing cell-specific cytotoxic effect of the SP94 ligands through localization of the cages to HepG2 cells. We previously observed similar result with a viral-capsid based delivery system.[39] These engineered AaLS not only incorporate drug molecules facilitating the solubilization of the drugs but also preserve the drug activity within the cancer cells, which might help effectively deliver the drugs to target cancer cells *in vivo*. Also, AaLS and other bacterial lumazine synthase have been used as vaccine delivery systems, which shows that lumazine synthase protein cage nanoparticles do not cause any significant immune response *in vivo*.[41, 42] However, *in vivo* immune alteration caused by AaLS and its bio-distribution should be thoroughly studied in the near future. Therefore, we have successfully demonstrated that AaLS can be used as a nanoscale modular template for constructing multifunctional theranostic systems with the capability of cell-specific targeted delivery of drugs and imaging probes simultaneously.

Conclusions

In this study, we developed the lumazine synthase (AaLS) as a versatile modular nanoplatform for the targeted delivery of diagnostic and/or therapeutic molecules depending on target cancer cells. The AaLS template acquired two different types of cell-specific targeting peptides, RGD4C and SP94 peptides, genetically and cargo molecules, either detecting molecules (NHS-fluorescein and F5M) or therapeutic molecules (AlDox and BTZ), chemically without disrupting the overall cage architecture. In fluorescence microscopy studies, fluorescently-labeled RGD4C- and SP94-AaLS individually exhibited specific binding capability toward KB cells and HepG2 cells, respectively, whereas AaLS without any targeting peptides did not. The MTT cell viability assay confirmed the enhanced cytotoxic effects of AlDox and BTZ delivered by RGD4C- and SP94-AaLS, respectively. In this work, we successfully demonstrate that the AaLS template has the genetic and chemical

plasticity that can be used to acquire diverse functions by design depending on their purposes. Thus, the AaLS is an excellent modular template for developing a versatile, multifunctional theranostic system, which has specific cell targeting ligands and diagnostic and therapeutic reagents simultaneously.

This work was supported by the National Research Foundation of Korea (NRF) grant funded by the Korean government (NRF-2013R1A1A1008228), the Collaborative Research Program for Convergence Technology (Seed-11-6) of the Korea (KRCF), and the year of 2014 research fund (1.140028.01) of UNIST.

Notes and references

[a]Department of Biological Sciences, School of Life Sciences, Ulsan National Institute of Science and Technology (UNIST), Ulsan, 689-798, Korea.
E-mail: sabsab7@unist.ac.kr; Fax: +82-52-217-5309; Tel: +82-52-217-5325

Electronic Supplementary Information (ESI) available: Experimental details and data for chemical conjugations of AaLS variants and *in vitro* binding and releasing assay of drug molecules are available. See DOI: 10.1039/c000000x/

1. D. Peer, J. M. Karp, S. Hong, O. C. Farokhzad, R. Margalit and R. Langer, *Nat. Nano.*, 2007, **2**, 751-760.
2. C. Sun, J. S. H. Lee and M. Zhang, *Adv. Drug Deliv. Rev.*, 2008, **60**, 1252-1265.
3. A. Rösler, G. W. M. Vandermeulen and H.-A. Klok, *Adv. Drug Deliv. Rev.*, 2012, **64**, 270-279.
4. J. Gong, M. Chen, Y. Zheng, S. Wang and Y. Wang, *J. Control. Release*, 2012, **159**, 312-323.
5. W. B. Liechty, D. R. Kryscio, B. V. Slaughter and N. A. Peppas, *Annu. Rev. Chem. Biomol. Eng.*, 2010, **1**, 149-173.
6. R. Haag and F. Kratz, *Angew. Chem. Int. Ed.*, 2006, **45**, 1198-1215.
7. A. Z. Wang, R. Langer and O. C. Farokhzad, *Annu. Rev. Med.*, 2012, **63**, 185-198.
8. T. M. Allen and P. R. Cullis, *Adv. Drug Deliv. Rev.*, 2013, **65**, 36-48.
9. A. A. Gabizon, *Clin. Cancer Res.*, 2001, **7**, 223-225.
10. A. MaHam, Z. Tang, H. Wu, J. Wang and Y. Lin, *Small*, 2009, **5**, 1706-1721.
11. Y. Ma, R. J. M. Nolte and J. J. L. M. Cornelissen, *Adv. Drug Deliv. Rev.*, 2012, **64**, 811-825.
12. K. Cho, X. Wang, S. Nie, Z. Chen and D. M. Shin, *Clini. Cancer Res.*, 2008, **14**, 1310-1316.
13. S. Aime, L. Frullano and S. Geninatti Crich, *Angew. Chem. Int. Ed.*, 2002, **41**, 1017-1019.
14. J.-A. Han, Y. J. Kang, C. Shin, J.-S. Ra, H.-H. Shin, S. Y. Hong, Y. Do and S. Kang, *Nanomedicine*, 2014, **10**, 561-569.
15. Y. J. Kang, H. J. Yang, S. Jeon, Y.-S. Kang, Y. Do, S. Y. Hong and S. Kang, *Macromol. Biosci.*, 2014, **14**, 619-625.
16. C. Kwon, Y. J. Kang, S. Jeon, S. Jung, S. Y. Hong and S. Kang, *Macromol. Biosci.*, 2012, **12**, 1452-1458.
17. M. Uchida, M. L. Flenniken, M. Allen, D. A. Willits, B. E. Crowley, S. Brumfield, A. F. Willis, L. Jackiw, M. Jutila, M. J. Young and T. Douglas, *J. Am. Chem. Soc.*, 2006, **128**, 16626-16633.
18. S.-H. Choi, I. C. Kwon, K. Y. Hwang, I.-S. Kim and H. J. Ahn, *Biomacromolecules*, 2011, **12**, 3099-3106.
19. M. L. Flenniken, L. O. Liepold, B. E. Crowley, D. A. Willits, M. J. Young and T. Douglas, *Chem. Commun.*, 2005, 447-449.
20. M. L. Flenniken, D. A. Willits, S. Brumfield, M. J. Young and T. Douglas, *Nano Lett.*, 2003, **3**, 1573-1576.
21. J. Min, H. Jung, H.-H. Shin, G. Cho, H. Cho and S. Kang, *Biomacromolecules*, 2013, **14**, 2332-2339.
22. J. Lucon, S. Qazi, M. Uchida, G. J. Bedwell, B. LaFrance, P. E. Prevelige and T. Douglas, *Nat. Chem.*, 2012, **4**, 781-788.
23. N. Stephanopoulos, G. J. Tong, S. C. Hsiao and M. B. Francis, *ACS Nano*, 2010, **4**, 6014-6020.
24. G. Destito, R. Yeh, C. S. Rae, M. G. Finn and M. Manchester, *Chem. Biol.*, 2007, **14**, 1152-1162.
25. Q. Zeng, H. Wen, Q. Wen, X. Chen, Y. Wang, W. Xuan, J. Liang and S. Wan, *Biomaterials*, 2013, **34**, 4632-4642.
26. D. Banerjee, A. P. Liu, N. R. Voss, S. L. Schmid and M. G. Finn, *ChemBioChem*, 2010, **11**, 1273-1279.
27. X. Zhang, W. Meining, M. Fischer, A. Bacher and R. Ladenstein, *J. Mol. Biol.*, 2001, **306**, 1099-1114.
28. X. Zhang, W. Meining, M. Cushman, I. Haase, M. Fischer, A. Bacher and R. Ladenstein, *J. Mol. Biol.*, 2003, **328**, 167-182.
29. F. P. Seebeck, K. J. Woycechowsky, W. Zhuang, J. P. Rabe and D. Hilvert, *J. Am. Chem. Soc.*, 2006, **128**, 4516-4517.
30. B. Wörsdörfer, Z. Pianowski and D. Hilvert, *J. Am. Chem. Soc.*, 2011, **134**, 909-911.
31. B. Wörsdörfer, K. J. Woycechowsky and D. Hilvert, *Science*, 2011, **331**, 589-592.
32. H. Moon, W. G. Kim, S. Lim, Y. J. Kang, H.-H. Shin, H. Ko, S. Y. Hong and S. Kang, *J. Mater. Chem. B*, 2013, **1**, 4504-4510.
33. R. Toita, M. Murata, S. Tabata, K. Abe, S. Narahara, J. S. Piao, J.-H. Kang and M. Hashizume, *Bioconjugate Chem.*, 2012, **23**, 1494-1501.
34. R. Toita, M. Murata, K. Abe, S. Narahara, J. S. Piao, J.-H. Kang and M. Hashizume, *Chem. Commun.*, 2013, **49**, 7442-7444.
35. D. Willner, P. A. Trail, S. J. Hofstead, H. D. King, S. J. Lasch, G. R. Braslawsky, R. S. Greenfield, T. Kaneko and R. A. Firestone, *Bioconjugate Chem.*, 1993, **4**, 521-527.
36. C. Ryppa, H. Mann-Steinberg, I. Fichtner, H. Weber, R. Satchi-Fainaro, M. L. Biniossek and F. Kratz, *Bioconjugate Chem.*, 2008, **19**, 1414-1422.
37. B. A. Teicher, G. Ara, R. Herbst, V. J. Palombella and J. Adams, *Clin. Cancer Res.*, 1999, **5**, 2638-2645.
38. D. Baiz, G. Pozzato, B. Dapas, R. Farra, B. Scaggiante, M. Grassi, L. Uxa, C. Giansante, C. Zennaro, G. Guarnieri and G. Grassi, *Biochimie*, 2009, **91**, 373-382.
39. J. Min, H. Moon, H. J. Yang, H.-H. Shin, S. Y. Hong and S. Kang, *Macromol. Biosci.*, 2014, **14**, 557-564.
40. J. Su, F. Chen, V. L. Cryns and P. B. Messersmith, *J. Am. Chem. Soc.*, 2011, **133**, 11850-11853.
41. E. Sciutto, A. Toledo, C. Cruz, G. Rosas, G. Meneses, D. Laplagne, N. Ainciart, J. Cervantes, G. Fragoso and F. A. Goldbaum, *Vaccine*, 2005, **23**, 2784-2790.
42. J.-S. Ra, H.-H. Shin, S. Kang and Y. Do, *Clin. Exp. Vaccine. Res.*, 2014, **3**, 227-234.

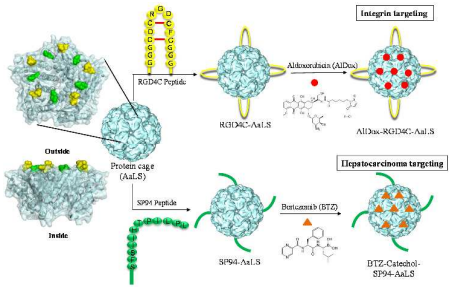

Lumazine synthase protein cage nanoparticle is developed as a modular delivery nanoplatform that delivers drugs to their target cancer cells.

A table of contents entry. This should include:

* Colour graphic: maximum size 8 cm x 4 cm

* Text: one sentence, of maximum 20 words, highlighting the novelty of the work